Since January 2020 Elsevier has created a COVID-19 resource centre with free information in English and Mandarin on the novel coronavirus COVID-19. The COVID-19 resource centre is hosted on Elsevier Connect, the company's public news and information website.

Journal of Hazardous Materials Letters 2 (2021) 100042

Contents lists available at ScienceDirect

Journal of Hazardous Materials Letters

journal homepage: www.sciencedirect.com/journal/journal-of-hazardous-materials-letters

Ethanol-based disinfectant sprays drive rapid changes in the chemical composition of indoor air in residential buildings

Jinglin Jiang [a,b], Xiaosu Ding [a], Kristofer P. Isaacson [c], Antonios Tasoglou [d], Heinz Huber [e], Amisha D. Shah [a,c], Nusrat Jung [a,*], Brandon E. Boor [a,b,*]

[a] Lyles School of Civil Engineering, Purdue University, West Lafayette, IN, United States
[b] Ray W. Herrick Laboratories, Center for High Performance Buildings, Purdue University, West Lafayette, IN, United States
[c] Division of Environmental and Ecological Engineering, Purdue University, West Lafayette, IN, United States
[d] RJ Lee Group Inc., Monroeville, PA, United States
[e] Edelweiss Technology Solutions, LLC, Novelty, OH, United States

ARTICLE INFO

Keywords:
Volatile organic compounds
Proton transfer reaction time-of-flight mass spectrometry
Building disinfection
Indoor contaminant mass transport
COVID-19 pandemic

ABSTRACT

The COVID-19 pandemic has resulted in increased usage of ethanol-based disinfectants for surface inactivation of SARS-CoV-2 in buildings. Emissions of volatile organic compounds (VOCs) and particles from ethanol-based disinfectant sprays were characterized in real-time (1 Hz) via a proton transfer reaction time-of-flight mass spectrometer (PTR-TOF-MS) and a high-resolution electrical low-pressure impactor (HR-ELPI+), respectively. Ethanol-based disinfectants drove sudden changes in the chemical composition of indoor air. VOC and particle concentrations increased immediately after application of the disinfectants, remained elevated during surface contact time, and gradually decreased after wiping. The disinfectants produced a broad spectrum of VOCs with mixing ratios spanning the sub-ppb to ppm range. Ethanol was the dominant VOC emitted by mass, with concentrations exceeding 10^3 μg m^{-3} and emission factors ranging from 10^1 to 10^2 mg g^{-1}. Listed and unlisted diols, monoterpenes, and monoterpenoids were also abundant. The pressurized sprays released significant quantities (10^4–10^5 cm^{-3}) of nano-sized particles smaller than 100 nm, resulting in large deposited doses in the tracheobronchial and pulmonary regions of the respiratory system. Inhalation exposure to VOCs varied with time during the building disinfection events. Much of the VOC inhalation intake (>60 %) occurred after the disinfectant was sprayed and wiped off the surface. Routine building disinfection with ethanol-based sprays during the COVID-19 pandemic may present a human health risk given the elevated production of volatile chemicals and nano-sized particles.

1. Introduction

The COVID-19 pandemic has led to the surging use of disinfectants for inactivation of SARS-CoV-2 (U.S. CDC, 2020; Pitol and Julian, 2021; Zheng et al., 2020). Ethanol (C_2H_6O) can inactivate human coronaviruses, including SARS-CoV-2 (Kratzel et al., 2020; Kumar et al., 2021; Meyers et al., 2021; Rabenau et al., 2005). Ethanol-based disinfectants have been widely used during the COVID-19 pandemic and are included in the U.S. EPA List N: Disinfectants for Coronavirus (U.S. EPA, 2020). Ethanol-based disinfection of buildings may pose a health risk due to inhalation exposure to ethanol and other volatile organic compounds (VOCs) included in the disinfectants.

Inhalation exposure to gas-phase ethanol is associated with adverse toxicological outcomes. Preclinical studies on animals revealed potential neural, hepatic, pulmonary, and cardiovascular risks of inhalation of ethanol and 2-propanol (Budygin et al., 2007; Hirth et al., 2016; Mouton et al., 2016). An increase of multiple biomarkers (BrAC, EtG, and EtS) was observed after use of alcohol-based hand sanitizers (1–3 pumps every 2−20 min) in several studies (Ahmed-Lecheheb et al., 2012; Ali et al., 2013; Arndt et al., 2014; Hautemanière et al., 2013a, 2013b). Inhalation of ethanol is of concern as it can be directly transmitted to the brain via arterial circulation, which may increase the risk of addiction (Maclean et al., 2017).

Given the diverse spectrum of ingredients included in commercial ethanol-based disinfectants, it is expected that such products can emit a wide range of VOCs. The human respiratory system, as the main route of

* Corresponding authors at: Lyles School of Civil Engineering, Purdue University, West Lafayette, IN, United States.
E-mail addresses: nusratj@purdue.edu (N. Jung), bboor@purdue.edu (B.E. Boor).

https://doi.org/10.1016/j.hazl.2021.100042

Available online 8 September 2021

VOC intake (Gong et al., 2017; Zhao et al., 2019), is at risk of impairment to pulmonary function when exposed to elevated VOC concentrations (Yoon et al., 2010; Zhao et al., 2019). Epidemiological studies have identified associations between inhalation exposure to VOCs and numerous respiratory diseases (Elliott et al., 2006; He et al., 2015). VOC exposures in residential and office buildings have been related to various adverse human health outcomes (Cakmak et al., 2014; Wolkoff et al., 2006). Pressurized sprays can also release sub-10 μm droplets and sub-100 nm particles; the composition of which is influenced by the spray product applied (Bekker et al., 2014; Hagendorfer et al., 2010; Jiang et al., 2021a; Nazarenko et al., 2011). Sub-100 nm particles can penetrate deep into the human respiratory system and result in adverse health outcomes, including respiratory and cardiovascular diseases (Heinzerling et al., 2016; Knibbs et al., 2011; Li et al., 2016; Oberdörster, 2000; Oberdörster et al., 2005; Stone et al., 2017; Weichenthal et al., 2007; Downward et al., 2018; Panas et al., 2014; Soppa et al., 2014).

Despite the potential exposure risks associated with increased use of disinfectant sprays during the COVID-19 pandemic, there is limited research characterizing the temporal emission profiles of such products. The objective of this study is to conduct real-time (1 Hz) emission measurements of gas- and particle-phase species released from ethanol-based disinfectants through use of a proton transfer reaction time-of-flight mass spectrometer (PTR-TOF-MS) and a high-resolution electrical low-pressure impactor (HR-ELPI+), respectively. Such state-of-the-art instrumentation enables improved temporal characterization of the fate and transport of potentially health hazardous materials in the indoor environment during building disinfection activities and associated inhalation exposures among occupants. To the authors' knowledge, this represents the first tandem application of a PTR-TOF-MS and HR-ELPI+ for real-time detection of VOCs and particles released from ethanol-based disinfectants.

2. Materials and methods

2.1. Study site: Purdue zero Energy Design Guidance for Engineers (zEDGE) Tiny House

The measurement campaign was conducted in a residential architectural engineering laboratory – the Purdue zero Energy Design Guidance for Engineers (zEDGE) Tiny House (Fig. S1). zEDGE is a mechanically ventilated single zone residential building with a conditioned interior volume of 60.35 m^3. A powered ventilator with a MERV 16 filter supplied filtered outdoor air to zEDGE (Fig. S2). zEDGE was maintained at a positive pressure (+9 Pa) with an outdoor air exchange rate (AER) of 3 h^{-1}. The details of the AER calculation are provided in the supplementary material. Two fans were used to promote mixing.

2.2. Protocol for ethanol-based disinfectant emission experiments

The disinfectant emission experiments were conducted on two 2 ft. × 3 ft. glass panels positioned on the kitchen countertop of zEDGE. The glass panels were used to isolate the indoor surface onto which the disinfectant was applied. A clean set of glass panels was used for each experiment. Two ethanol-based disinfectant sprays included in List N were evaluated (products A, B). An ingredient summary is provided in Table S1. Products A and B contained ethanol at 30–60 %wt. and 58 % wt., respectively. Both sprays utilized alkanes as propellants (A, B: propane (C_3H_8), A: isobutane (i-C_4H_{10}), B: n-butane (n-C_4H_{10})) and included fragrances. Product B incorporated triethylene glycol ($C_6H_{14}O_4$) as an additional disinfectant at 6 %wt. n-Alkyl dimethyl benzyl ammonium saccharinate was present in both sprays (≤0.2 %wt.), however, it was not detected in the gas-phase.

Three experiments were completed per disinfectant (A: A1, A2, A3 and B: B1, B2, B3). Each experiment was conducted in three periods over 80 min (Fig. S3). The first period included 10 min of background measurements. The second period included 10 min of surface contact for the disinfectant that began with a spray event. 24 sprays were applied to the glass panels in a matrix with 3 rows and 8 columns at about 1 ft. above the surface. At the end of the second period, the liquid film of disinfectant was removed via wiping with two absorbent towels (removed from zEDGE after wiping). The third period included a 60 min concentration decay. zEDGE was occupied by one researcher during the spray and wipe events and unoccupied for the remaining periods. The disinfectants were used as prescribed by the manufacturer.

2.3. Real-time measurement of VOCs via PTR-TOF-MS and particles via HR-ELPI+

Mixing ratios of VOCs were measured at 1 Hz by a PTR-TOF-MS (PTR-TOF 4000, Ionicon Analytic Ges.m.b.H, Innsbruck, Austria) using hydronium (H_3O^+) as the reagent ion. In the drift tube, molecules with proton affinities greater than that of water (691 kJ mol^{-1}) will collide with H_3O^+ and be ionized through a proton transfer reaction (Blake et al., 2009; Lindinger et al., 1998). The ionized molecules are then detected by a TOF-MS. Mass spectra for mass-to-charge ratios (m/z) from 20 to 450 were recorded. Pressure, voltage, and temperature for the drift tube were set at 2.2 mbar, 600 V, and 70 °C respectively, maintaining the ionization field energy (E/N) at approximately 139 Td. The abundance of impurity ions (O_2^+, NO^+) was <10 %. The sampling inlet was located near the center of the zEDGE kitchen. A PFA tube (3/8 in. OD) was used as the sampling line. At the intake of the sampling line, a PTFE membrane filter (1 μm pore size) was installed to remove particles. The exhaust from the PTR-TOF-MS was directed outdoors. The PTR-TOF-MS was calibrated daily using two VOC gas standard mixtures (Table S2). Mixing ratios of VOCs not included in the gas standards were calculated based on proton transfer reaction theory (de Gouw and Warneke, 2007; Klein et al., 2018). Reaction rate constants were derived from the literature if available (Pagonis et al., 2019), otherwise 2×10^{-9} cm^3 s^{-1} was used (Table S3). Given the large number of ions detected by the PTR-TOF-MS during the disinfection events, only the ions that increased by >50 % beyond their average background mixing ratios and peaked at >0.1 ppb are reported. A material balance model was used to estimate ethanol emission factors (EFs, mg g^{-1} or mg ml^{-1}), as described in the supplementary material.

Particle size distributions from 6 to 10000 nm in aerodynamic diameter (D_a) were measured at 1 Hz with a HR-ELPI+ (Dekati Ltd., Kangasala, Finland). The aerodynamic diameter of an irregularly shaped particle is the diameter of a spherical particle with a density of 1 g cm^{-3} and the same settling velocity as the irregularly shaped particle (Hinds, 1999). The HR-ELPI+ sampled air near the center of the zEDGE kitchen. Oil-soaked sintered collection plates were used to eliminate particle bounce and impactor overloading. Details on the operational principle of the ELPI+ can be found elsewhere (Järvinen et al., 2014; Lemmetty et al., 2005; Marjamäki et al., 2000; Marjamäki et al., 2005). The HR-ELPI+ uses an iterative inversion algorithm to improve the size-resolution beyond the standard ELPI+ (Saari et al., 2018). The exhaust of the HR-ELPI+ pump was directed outdoors via the bathroom exhaust (Fig. S2). Measured particle number size distributions (dN/dLog (D_a), cm^{-3}) were translated to particle mass size distributions (dM/dLog (D_a), μg m^{-3}) assuming spherical particles with a density of 1 g cm^{-3} for D_a≤100 nm (Wu and Boor, 2020) and the density of the disinfectant solution for particles with D_a>100 nm, which were likely generated by the spray process (Table S1). The particle number size distributions were used to estimate number respiratory tract deposited doses for the head airways, tracheobronchial region, and pulmonary region, as described in the supplementary material.

3. Results and discussion

3.1. Temporal VOC emission profiles during ethanol-based disinfection events in buildings

The use of ethanol-based disinfectants in buildings results in sudden changes in the chemical composition of indoor air. Products A and B emitted a complex mixture of VOCs. More than 50 ions were found to increase by >50 % relative to background, with individual ion mixing ratios spanning the sub-ppb to ppm range (Tables S4–S5). Detected ions were assigned to one of the following VOC categories: (1.) ethanol and ethanol cluster ions; (2.) listed fragrance compounds for product B; and (3.) compounds associated with essential oils. Remaining ions with identified ion formulas were categorized as: (4.) hydrocarbons (C_xH_y); (5.) oxygenated hydrocarbons ($C_xH_yO_z$); and (6.) nitriles (C_xH_yN) for product B. Signals without identified formulas were reported as: (7.) unidentified. Experiments A2 and B1 were selected as case studies for each product. The real-time PTR-TOF-MS data was visualized in two forms: time-series of ion-resolved mixing ratios (Fig. 1(I.a., II.a.)) and time-series of categorized VOC mass concentrations (Fig. 2). Figs. S4–S11 show results for other experiments.

Several of the detected ions are associated with ethanol. *m/z* 47.06 ($C_2H_7O^+$) is the parent ion of ethanol. *m/z* 45.03 ($C_2H_5O^+$), *m/z* 65.06 ($C_2H_7O^+{\cdot}(H_2O)$), *m/z* 75.08 ($C_2H_5^+{\cdot}(C_2H_6O)$), *m/z* 93.10 ($C_2H_7O^+{\cdot}(C_2H_6O)$), and *m/z* 139.12 ($C_2H_7O^+{\cdot}(C_2H_6O)_2$) are fragment or cluster ions of ethanol (Boscaini et al., 2004; Buhr et al., 2002). The formation of ethanol cluster ions in the drift tube of the PTR-TOF-MS at high ethanol mixing ratios, such as those observed here, is described in detail by Boscaini et al. (2004). The increase of *m/z* 31.02 (CH_3O^+) may be due to reactions between ethanol and O_2^+ impurity ions in the drift tube (Kushch et al., 2008; Schripp et al., 2010; Španěl and Smith, 2008). Ethanol can react with the hydroxyl radical and nitric oxide to form formaldehyde (CH_2O) and acetaldehyde (C_2H_4O), which are detected at *m/z* 31.02 and *m/z* 45.03, respectively (Dunmore et al., 2016). However, the PTR-TOF-MS cannot separate isomers and fragment ions of different origins; thus, the potential indoor formation of formaldehyde and acetaldehyde cannot be evaluated. Real-time separation of isomers requires a PTR-TOF-MS configured with a fast gas chromatograph

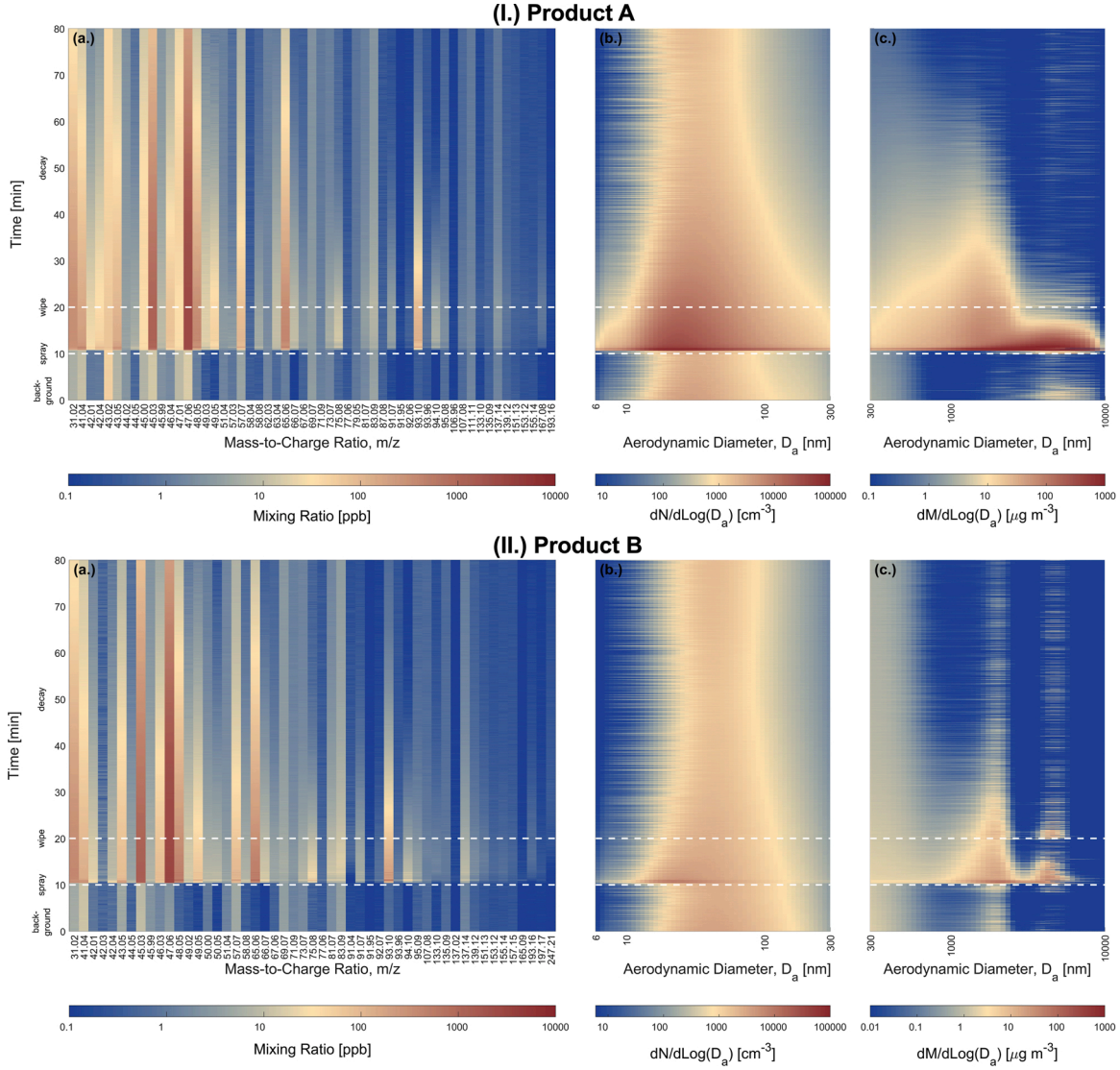

Fig. 1. (I.) Time-series for ethanol-based disinfection event A2 using product A. (a.) ion-resolved mixing ratios from *m/z* 31 to 193, (b.) particle number size distributions from $D_a = 6$ to 300 nm, and (c.) particle mass size distributions from $D_a = 300$ to 10000 nm. (II.) Time-series for ethanol-based disinfection event B1 using product B. (a.) ion-resolved mixing ratios from *m/z* 31 to 247, (b.) particle number size distributions from $D_a = 6$ to 300 nm, and (c.) particle mass size distributions from $D_a = 300$ to 10000 nm. Additional details on the detected ions can be found in Table S3. Peak and average background mixing ratios for each ion can be found in Tables S4–S5. Peak and average background particle number and mass concentrations can be found in Table S6.

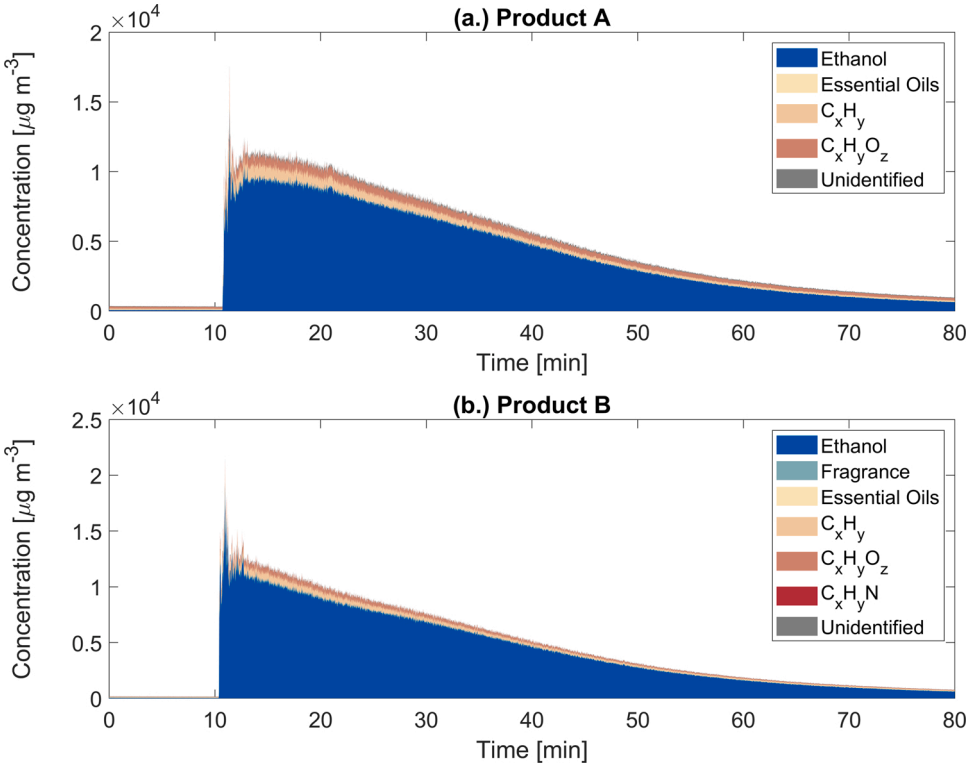

Fig. 2. Time-series of the categorized VOC mass concentrations during: (a.) ethanol-based disinfection event A2 using product A and (b.) ethanol-based disinfection event B1 using product B. Detected ions associated with each VOC category can be found in Table S3.

(Claflin et al., 2021).

During experiment A2, the ethanol mass concentration increased immediately after the disinfectant was applied, reaching a peak at 14.64 mg m^{-3} (6575 ppb), 200-fold greater than background levels (0.073 mg m^{-3}, Table S4) (Figs. 1(I.a.) and 2 (a.)). Ethanol concentrations remained elevated during the 10 min surface contact time, after which they gradually decayed following removal of the disinfectant residue from the glass panels. However, the ethanol mass concentration remained at 0.62 mg m^{-3} (326 ppb) at the end of the 60 min decay period, 9-fold greater than background. A similar temporal emission profile was observed during experiment B1, where the ethanol mass concentration peaked at 18.97 mg m^{-3} (7983 ppb), 600-fold greater than background (0.034 mg m^{-3}, Table S5) (Figs. 1(II.a.) and 2 (b.)). Ethanol was the dominant VOC released from both disinfectant sprays by mass (Fig. 2). This is due in part to the abundance of ethanol in the disinfectant solutions (A: 30–60 %wt., B: 58 %wt.) and the high volatility of ethanol (Salthammer, 2016). The mean ethanol EFs for disinfectants A and B were 99.32 mg g^{-1} (82.54 mg ml^{-1}) and 32.31 mg g^{-1} (26.17 mg ml^{-1}), respectively (Table S7). This suggests that disinfection activities are important episodic indoor sources of ethanol.

In addition to ethanol, the PTR-TOF-MS measurements revealed the presence of a myriad of VOCs in the disinfectant emissions; their temporal emission profiles can be seen in Figs. 1 and 2. While product A did not specify fragrance ingredients, monoterpenes and monoterpenoids related to essential oils were detected by the PTR-TOF-MS (Angulo Milhem et al., 2020; Nematollahi et al., 2018); this enables characterization of the unlisted fragrances in the disinfectant. Mixing ratios of monoterpenes ($C_{10}H_{16}$, detected at *m/z* 81.07 ($C_6H_9^+$) and *m/z* 137.14 ($C_{10}H_{17}^+$)) peaked at 10.7 ppb after applying product A. Monoterpenoids detected at *m/z* 151.13 ($C_{10}H_{15}O^+$, possibly thymol or carvone), *m/z* 153.12 ($C_{10}H_{17}O^+$, possibly camphor or citral), *m/z* 155.13 ($C_{10}H_{19}O^+$, possibly linalool, eucalyptol, citronellal, α-terpineol, or terpinen-4-ol), and *m/z* 193.16 ($C_{13}H_{21}O^+$, possibly ionone or damascone) are components of essential oils (Babu et al., 2002; Kokkini et al., 1995; Msaada et al., 2007; Wang et al., 2009). Their mixing ratios increased 2.7-4.2-fold above background, but were relatively low in magnitude, with peaks ranging from 0.33-0.76 ppb. Many of the listed fragrance components for product B (>0.01 %wt. or on a designated list) were detected by the PTR-TOF-MS. *m/z* 135.09 ($C_6H_{15}O_3^+$, dipropylene glycol), *m/z* 137.14 ($C_{10}H_{17}^+$, 3-carene, also detected at *m/z* 81.07), *m/z* 157.15 ($C_{10}H_{21}O^+$, dihydromyrcenol), *m/z* 165.09 ($C_{10}H_{13}O_2^+$, eugenol), *m/z* 197.17 ($C_{12}H_{21}O_2^+$, linalyl acetate), and *m/z* 247.21 ($C_{17}H_{27}O^+$, acetyl cedrene) reached peak mixing ratios 2.6-18.2-fold greater than background. Several unlisted monoterpenoids were also observed (*m/z* 151.13, *m/z* 153.12, *m/z* 155.13, and *m/z* 193.16). Their mixing ratios were 4.1-12.1-fold greater than background, however, peak mixing ratios were low (1.0–1.6 ppb). Monoterpenes and monoterpenoids are common fragrance ingredients in disinfectants and could cause occupational asthma (Malo and Chan-Yeung, 2009; Melchior Gerster et al., 2014; Vizcaya Fernández et al., 2011).

Emissions from the two ethanol-based disinfectants led to significant increases in the mixing ratios (typ. 100−450 ppb) of *m/z* 42.04 ($C_3H_6^+$), *m/z* 43.05 ($C_3H_7^+$), and *m/z* 57.07 ($C_4H_9^+$). These ions can be attributed to the high abundance of alkanes (often ≥5 %wt.) included in the sprays as propellants (Dinh et al., 2015). $C_3H_6^+$, $C_3H_7^+$, and $C_4H_9^+$ can be formed due to reactions between i-C_4H_{10} and n-C_4H_{10} with O_2^+ impurity ions (Španěl and Smith, 1998; Wilson et al., 2003). Similarly, $C_3H_7^+$ can be formed via reactions between C_3H_8 and O_2^+ and NO^+ impurity ions. While i-C_4H_{10} and n-C_4H_{10} have low proton affinities (677.8 kJ mol^{-1}), it has been shown they undergo slow association reactions with H_3O^+ to form $C_4H_9^+$ (Wilson et al., 2003). Due to such reactions with H_3O^+ reagent ions and O_2^+ and NO^+ impurity ions, PTR-TOF-MS measurements in the indoor environment are therefore sensitive to episodic emissions of C_3-C_4 alkanes from pressurized spray-based consumer products. This precludes identification of selected ingredients in the disinfectants, such as triethylene glycol and t-butanol, that have a major fragment at *m/z* 57.07 (Pagonis et al., 2019). Several unlisted diols were also detected by the PTR-TOF-MS, including methanediol (*m/z* 49.03), 1,2-ethanediol

(*m/z* 63.04), 1,2-propanediol (*m/z* 77.06), 1,4-butanediol (*m/z* 91.07), and diethylene glycol (*m/z* 107.08). Peak mixing ratios for most were between 1−10 ppb, with methanediol the most abundant at 18−28 ppb.

3.2. Temporal particle emission profiles during ethanol-based disinfection events in buildings

Application of ethanol-based disinfectant sprays was associated with a significant increase in indoor particle number (PN) and particle mass (PM) concentrations (Table S6). The temporal evolution in particle number and mass size distributions during disinfection events A2 and B1 are illustrated in Fig. 1(I.b., II.b.) and (I.c., II.c.). The HR-ELPI+ measurements revealed substantial formation of nano-sized particles with $D_a \leq 100$ nm (modal $D_a \sim 23$ nm) immediately after application of product A. Peak PN concentrations ranged from 8.3 to 11.5 × 10^4 cm^{-3}, similar in magnitude to PN concentrations observed during cooking on gas and electric stoves (Jiang et al., 2021b). Product A also produced accumulation and coarse mode particles from $D_a = 300-10000$ nm that dominated particle mass size distributions. $PM_{2.5}$ and PM_{10} concentrations built up rapidly to 706 μg m^{-3} and 2708 μg m^{-3}, respectively. Product B produced fewer particles compared to A. The variation in particle emissions among the two products may be due to differences in the spray nozzles (Nuyttens et al., 2007) and the composition of the disinfectant solutions (Kim et al., 2020). The observed particles are likely disinfectant droplets formed by the propellant spray process (Bekker et al., 2014; Hagendorfer et al., 2010).

Indoor production of nano-sized particles on the order of 10^4-10^5 cm^{-3} by the ethanol-based disinfectant sprays resulted in number respiratory tract deposited doses of 10^8-10^9 particles for an adult during the spray and contact periods (Table S8). Much of the number dose was received in the tracheobronchial and pulmonary regions. Such sprays may present a human health risk as inhalation of sub-100 nm particles is associated with numerous adverse toxicological outcomes (Allen et al., 2017; Hussein et al., 2020; Li et al., 2016; Stone et al., 2017).

3.3. Human inhalation exposure to VOCs during ethanol-based disinfection events in buildings

High-resolution VOC measurements with a PTR-TOF-MS enables evaluation of real-time human inhalation exposure to VOC emissions during and after application of ethanol-based disinfectants. Inhalation exposure was evaluated for an adult involved in an indoor disinfection event following the temporal sequence of the experiments: 2 min spray period, 8 min contact period, 2 min wipe period, and 58 min decay period. Fig. 3 illustrates the per-period inhalation intake of VOCs for events A2 and B1. Figs. S12–S15 show results for other experiments. Ethanol contributed 80 % and 83 % to the total VOC inhalation intake during disinfection events A2 and B1, respectively. A non-negligible fraction (>15 %) of the total VOC inhalation intake was attributed to the remaining VOC categories (Fig. 3). Thus, one will inhale a complex mixture of VOCs during application of ethanol-based disinfectants. The magnitude of the total VOC mass inhaled (7−8 mg) presents a health risk for those involved in routine building disinfection during the COVID-19 pandemic.

The PTR-TOF-MS revealed time-dependent variations in VOC inhalation intake during the disinfection events. The spray, contact, wipe, and decay periods contributed 3 %, 24 %, 6 %, and 67 % to the total VOC inhalation intake (7.54 mg) during the 70 min disinfection event A2,

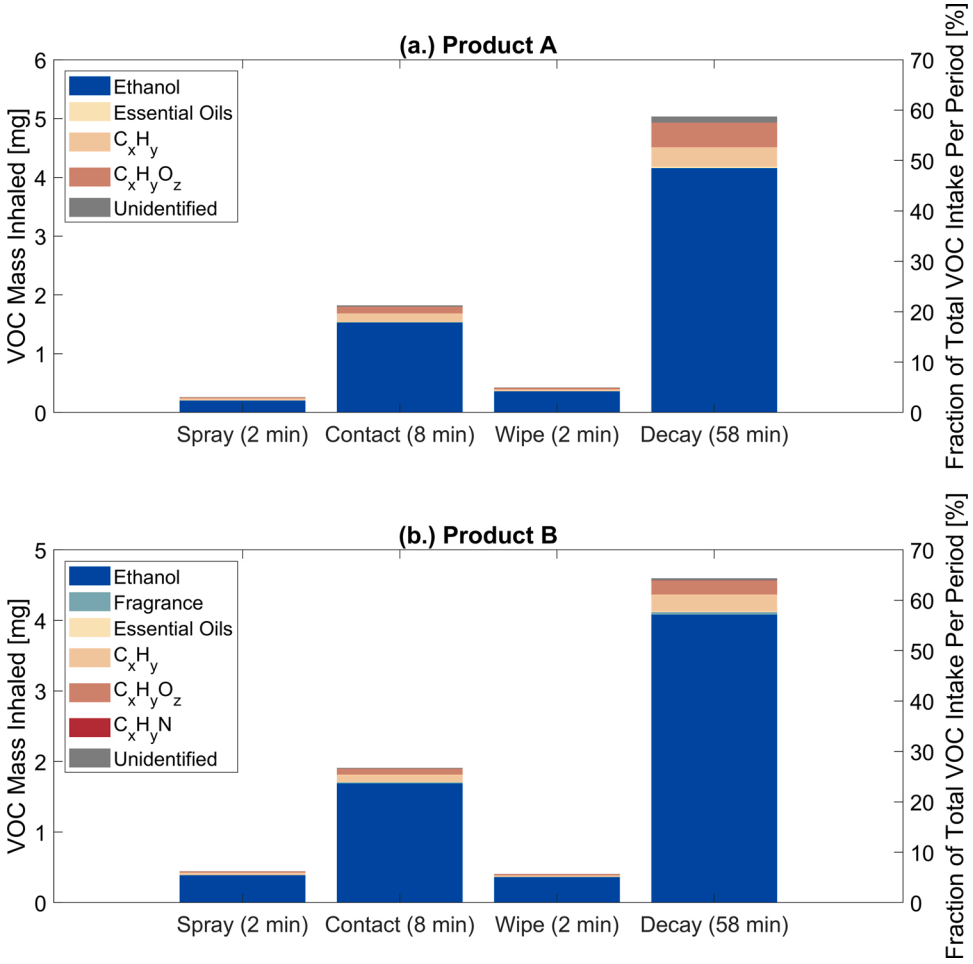

Fig. 3. Inhalation exposure assessment during: (a.) ethanol-based disinfection event A2 using product A: (left y-axis) inhalation intake of the categorized VOCs during the spray, contact, wipe, and decay periods and (right y-axis) fraction of the total VOC inhalation intake per period; and (b.) ethanol-based disinfection event B1 using product B: (left y-axis) inhalation intake of the categorized VOCs during the spray, contact, wipe, and decay periods and (right y-axis) fraction of the total VOC inhalation intake per period. Inhalation exposure is evaluated for an adult engaged in light activity with an inhalation rate of 1.25 m^3 h^{-1} (U.S. EPA, 2011). Detected ions associated with each VOC category can be found in Table S3.

respectively. This is comparable to that of disinfection event B1 (6 %, 26 %, 6 %, and 62 %). zEDGE was equipped with a powered ventilator that maintained an outdoor AER of 3 h^{-1}; this aided in diluting VOCs released by the disinfectants. However, it can be observed that VOC mass concentrations remained elevated during the entirety of the decay period as compared to background (Figs. 1 and 2). The VOC inhalation intake during the decay period was significant, contributing >60 % to the total intake. A person remaining in the same indoor space they disinfected for one hour following completion of the disinfection procedure would inhale a greater VOC mass than during the disinfection procedure itself.

4. Conclusions

This study demonstrated that a PTR-TOF-MS and HR-ELPI+ can be used together for real-time indoor detection of gas- and particle-phase species during residential building disinfection activities. Ethanol-based disinfectant sprays emitted a complex multi-phase mixture that included a broad spectrum of VOCs and particles. Notably, the disinfectants released significant quantities of ethanol (6000−8000 ppb) and nano-sized particles (10^4-10^5 cm^{-3}) to the indoor environment. Inhalation exposure was strongly time-dependent, with the majority of VOC inhalation intake occurring in the one hour period after the disinfectant was sprayed and wiped off the surface. Given the increased use of ethanol-based disinfectants during the COVID-19 pandemic, there is an urgent need to understand the health risks of exposure to elevated concentrations of VOCs and particles produced by such products. As shown in this study, PTR-TOF-MS and HR-ELPI+ measurements can characterize the emissions of potentially health hazardous materials released from disinfectant sprays.

Declaration of Competing Interest

The authors declare that they have no conflict of interest.

Acknowledgements

Financial support was provided by a Protect Purdue Innovations Faculty Grant (to N.J., B.E.B, and A.D.S) and the National Science Foundation (CBET-1847493 to B.E.B.). The authors are thankful for the support of Danielle N. Wagner, Jun Ho Kim, and David Rater of the Lyles School of Civil Engineering at Purdue University.

Appendix A. Supplementary material

Supplementary material related to this article can be found, in the online version, at doi:https://doi.org/10.1016/j.hazl.2021.100042.

References

Ahmed-Lecheheb, D., Cunat, L., Hartemann, P., Hautemanière, A., 2012. Dermal and pulmonary absorption of ethanol from alcohol-based hand rub. J. Hosp. Infect. 81, 31–35. https://doi.org/10.1016/j.jhin.2012.02.006.

Ali, S.S., Wilson, M.P., Castillo, E.M., Witucki, P., Simmons, T.T., Vilke, G.M., 2013. Common hand sanitizer may distort readings of breathalyzer tests in the absence of acute intoxication. Academic Emergency Medicine. John Wiley & Sons, Ltd, pp. 212–215. https://doi.org/10.1111/acem.12073.

Allen, J.L., Oberdorster, G., Morris-Schaffer, K., Wong, C., Klocke, C., Sobolewski, M., Conrad, K., Mayer-Proschel, M., Cory-Slechta, D.A., 2017. Developmental neurotoxicity of inhaled ambient ultrafine particle air pollution: parallels with neuropathological and behavioral features of autism and other neurodevelopmental disorders. NeuroToxicology 59, 140–154. https://doi.org/10.1016/j.neuro.2015.12.014.

Angulo Milhem, S., Verriele, M., Nicolas, M., Thevenet, F., 2020. Indoor use of essential oil-based cleaning products: emission rate and indoor air quality impact assessment based on a realistic application methodology. Atmos. Environ. https://doi.org/10.1016/j.atmosenv.2020.118060.

Arndt, T., Schröfel, S., Güssregen, B., Stemmerich, K., 2014. Inhalation but not transdermal resorption of hand sanitizer ethanol causes positive ethyl glucuronide findings in urine. For. Sci. Int. 237, 126–130. https://doi.org/10.1016/j.forsciint.2014.02.007.

Babu, K.G.D., Singh, B., Joshi, V.P., Singh, V., 2002. Essential oil composition of Damask rose (Rosa damascena Mill.) distilled under different pressures and temperatures. Flavour Fragr. J. 17, 136–140. https://doi.org/10.1002/ffj.1052.

Bekker, C., Brouwer, D.H., van Duuren-Stuurman, B., Tuinman, I.L., Tromp, P., Fransman, W., 2014. Airborne manufactured nano-objects released from commercially available spray products: temporal and spatial influences. J. Exp. Sci. Environ. Epidemiol. 24, 74–81. https://doi.org/10.1038/jes.2013.36.

Blake, R.S., Monks, P.S., Ellis, A.M., 2009. Proton-transfer reaction mass spectrometry. Chem. Rev. https://doi.org/10.1021/cr800364q.

Boscaini, E., Mikoviny, T., Wisthaler, A., Hartungen, Evon, Märk, T.D., 2004. Characterization of wine with PTR-MS. Int. J. Mass Spectr. 239, 215–219. https://doi.org/10.1016/j.ijms.2004.07.023.

Budygin, E.A., Oleson, E.B., Mathews, T.A., Läck, A.K., Diaz, M.R., McCool, B.A., Jones, S.R., 2007. Effects of chronic alcohol exposure on dopamine uptake in rat nucleus accumbens and caudate putamen. Psychopharmacology 193, 495–501. https://doi.org/10.1007/s00213-007-0812-1.

Buhr, K., van Ruth, S., Delahunty, C., 2002. Analysis of volatile flavour compounds by Proton Transfer Reaction-Mass Spectrometry: fragmentation patterns and discrimination between isobaric and isomeric compounds. Int. J. Mass Spectr. 221, 1–7. https://doi.org/10.1016/S1387-3806(02)00896-5.

Cakmak, S., Dales, R.E., Liu, L., Kauri, L.M., Lemieux, C.L., Hebbern, C., Zhu, J., 2014. Residential exposure to volatile organic compounds and lung function: results from a population-based cross-sectional survey. Environ. Pollut. 194, 145–151. https://doi.org/10.1016/j.envpol.2014.07.020.

Centers for Disease Control and Prevention (CDC), 2020. Guidance for Cleaning and Disinfecting Public Spaces, Workplaces, Businesses, Schools, and Homes | CDC [WWW Document]. URL https://www.cdc.gov/coronavirus/2019-ncov/community/reopen-guidance.html (Accessed 1.20.21).

Claflin, M.S., Pagonis, D., Finewax, Z., Handschy, Av., Day, D.A., Brown, W.L., Jayne, J. T., Worsnop, D.R., Jimenez, J.L., Ziemann, P.J., de Gouw, J., Lerner, B.M., 2021. An in situ gas chromatograph with automatic detector switching between PTR-and EI-TOF-MS: isomer-resolved measurements of indoor air. Atmos. Meas. Tech. 14, 133–152. https://doi.org/10.5194/amt-14-133-2021.

de Gouw, J., Warneke, C., 2007. Measurements of volatile organic compounds in the earth's atmosphere using proton-transfer-reaction mass spectrometry. Mass Spectr. Rev. https://doi.org/10.1002/mas.20119.

Dinh, T.V., Kim, S.Y., Son, Y.S., Choi, I.Y., Park, S.R., Sunwoo, Y., Kim, J.C., 2015. Emission characteristics of VOCs emitted from consumer and commercial products and their ozone formation potential. Environ. Sci. Pollut. Res. 22, 9345–9355. https://doi.org/10.1007/s11356-015-4092-8.

Downward, G.S., van Nunen, E.J.H.M., Kerckhoffs, J., Vineis, P., Brunekreef, B., Boer, J. M.A., Messier, K.P., Roy, A., Verschuren, W.M.M., van der Schouw, Y.T., Sluijs, I., Gulliver, J., Hoek, G., Vermeulen, R., 2018. Long-term exposure to ultrafine particles and incidence of cardiovascular and cerebrovascular disease in a prospective study of a Dutch cohort. Environ. Health Perspect. 126, 127007 https://doi.org/10.1289/EHP3047.

Dunmore, R.E., Whalley, L.K., Sherwen, T., Evans, M.J., Heard, D.E., Hopkins, J.R., Lee, J.D., Lewis, A.C., Lidster, R.T., Rickard, A.R., Hamilton, J.F., 2016. Atmospheric ethanol in London and the potential impacts of future fuel formulations. Faraday Discus. 189, 105–120. https://doi.org/10.1039/c5fd00190k.

Elliott, L., Longnecker, M.P., Kissling, G.E., London, S.J., 2006. Volatile organic compounds and pulmonary function in the Third National Health and Nutrition Examination Survey, 1988–1994. Environ. Health Perspect. 114, 1210–1214. https://doi.org/10.1289/ehp.9019.

Gong, Y., Wei, Y., Cheng, J., Jiang, T., Chen, L., Xu, B., 2017. Health risk assessment and personal exposure to Volatile Organic Compounds (VOCs) in metro carriages—A case study in Shanghai, China. Sci. Total Environ. 574, 1432–1438. https://doi.org/10.1016/j.scitotenv.2016.08.072.

Hagendorfer, H., Lorenz, C., Kaegi, R., Sinnet, B., Gehrig, R., Goetz, N.V., Scheringer, M., Ludwig, C., Ulrich, A., 2010. Size-fractionated characterization and quantification of nanoparticle release rates from a consumer spray product containing engineered nanoparticles. J. Nanopart. Res. 12, 2481–2494. https://doi.org/10.1007/s11051-009-9816-6.

Hautemanière, A., Ahmed-Lecheheb, D., Cunat, L., Hartemann, P., 2013a. Assessment of transpulmonary absorption of ethanol from alcohol-based hand rub. Am. J. Infect. Control 41. https://doi.org/10.1016/j.ajic.2012.09.004.

Hautemanière, A., Cunat, L., Ahmed-Lecheheb, D., Hajjard, F., Gerardin, F., Morele, Y., Hartemann, P., 2013b. Assessment of exposure to ethanol vapors released during use of Alcohol-Based Hand Rubs by healthcare workers. J. Infect. Public Health 6, 16–26. https://doi.org/10.1016/j.jiph.2012.09.015.

Heinzerling, A., Hsu, J., Yip, F., 2016. Respiratory health effects of ultrafine particles in children: a literature review. Water, Air, Soil Pollut. 227, 1–21. https://doi.org/10.1007/s11270-015-2726-6.

He, Z., Li, G., Chen, J., Huang, Y., An, T., Zhang, C., 2015. Pollution characteristics and health risk assessment of volatile organic compounds emitted from different plastic solid waste recycling workshops. Environ. Int. 77, 85–94. https://doi.org/10.1016/j.envint.2015.01.004.

Hinds, W.C., 1999. Aerosol Technology: Properties, Behavior, and Measurement of Airborne Particles, 2nd Edition. Wiley.

Hirth, N., Meinhardt, M.W., Noori, H.R., Salgado, H., Torres-Ramirez, O., Uhrig, S., Broccoli, L., Vengeliene, V., Roßmanith, M., Perreau-Lenz, S., Köhr, G., Sommer, W. H., Spanagel, R., Hansson, A.C., 2016. Convergent evidence from alcohol-dependent humans and rats for a hyperdopaminergic state in protracted abstinence. Proc. Natl. Acad. Sci. U. S. A. 113, 3024–3029. https://doi.org/10.1073/pnas.1506012113.

Hussein, T., Boor, B.E., Löndahl, J., 2020. Regional inhaled deposited dose of indoor combustion-generated aerosols in Jordanian urban homes. Atmosphere 11, 1150. https://doi.org/10.3390/atmos11111150.

Järvinen, A., Aitomaa, M., Rostedt, A., Keskinen, J., Yli-Ojanperä, J., 2014. Calibration of the new electrical low pressure impactor (ELPI+). J. Aerosol Sci. 69, 150–159. https://doi.org/10.1016/j.jaerosci.2013.12.006.

Jiang, J., Ding, X., Tasoglou, A., Huber, H., Shah, A.D., Jung, N., Boor, B.E., 2021a. Real-time measurements of botanical disinfectant emissions, transformations, and multiphase inhalation exposures in buildings. Environ. Sci. Technol. Lett. 8, 558–566. https://doi.org/10.1021/ACS.ESTLETT.1C00390.

Jiang, J., Jung, N., Boor, B.E., 2021b. Using building energy and smart thermostat data to evaluate indoor ultrafine particle source and loss processes in a net-zero energy house. ACS ES&T Eng. 1, 780–793. https://doi.org/10.1021/acsestengg.1c00002.

Kim, T., Park, J., Seo, J., Yoon, H., Lee, B., Lim, H., Lee, D., Kim, P., Yoon, C., Lee, K., Zoh, K.D., 2020. Behavioral characteristics to airborne particles generated from commercial spray products. Environ. Int. 140, 105747 https://doi.org/10.1016/j.envint.2020.105747.

Klein, F., Pieber, S.M., Ni, H., Stefenelli, G., Bertrand, A., Kilic, D., Pospisilova, V., Temime-Roussel, B., Marchand, N., el Haddad, I., Slowik, J.G., Baltensperger, U., Cao, J., Huang, R.J., Prévôt, A.S.H., 2018. Characterization of gas-phase organics using proton transfer reaction time-of-flight mass spectrometry: residential coal combustion. Environ. Sci. Technol. 52, 2612–2617. https://doi.org/10.1021/acs.est.7b03960.

Knibbs, L.D., Cole-Hunter, T., Morawska, L., 2011. A review of commuter exposure to ultrafine particles and its health effects. Atmos. Environ. 45, 2611–2622. https://doi.org/10.1016/j.atmosenv.2011.02.065.

Kokkini, S., Karousou, R., Lanaras, T., 1995. Essential oils of spearmint (Carvone-rich) plants from the island of Crete (Greece). Biochem. Syst. Ecol. 23, 425–430. https://doi.org/10.1016/0305-1978(95)00021-L.

Kratzel, A., Todt, D., V'kovski, P., Steiner, S., Gultom, M., Thao, T.T.N., Ebert, N., Holwerda, M., Steinmann, J., Niemeyer, D., Dijkman, R., Kampf, G., Drosten, C., Steinmann, E., Thiel, V., Pfaender, S., 2020. Inactivation of severe acute respiratory syndrome coronavirus 2 by WHO-recommended hand rub formulations and alcohols. Emerg. Infect. Dis. 26, 1592–1595. https://doi.org/10.3201/eid2607.200915.

Kumar, M., Mazumder, P., Mohapatra, S., Kumar Thakur, A., Dhangar, K., Taki, K., Mukherjee, S., Kumar Patel, A., Bhattacharya, P., Mohapatra, P., Rinklebe, J., Kitajima, M., Hai, F.I., Khursheed, A., Furumai, H., Sonne, C., Kuroda, K., 2021. A chronicle of SARS-CoV-2: seasonality, environmental fate, transport, inactivation, and antiviral drug resistance. J. Hazard. Mater. 405, 124043 https://doi.org/10.1016/j.jhazmat.2020.124043.

Kushch, I., Schwarz, K., Schwentner, L., Baumann, B., Dzien, A., Schmid, A., Unterkofler, K., Gastl, G., Španěl, P., Smith, D., Amann, A., 2008. Compounds enhanced in a mass spectrometric profile of smokers' exhaled breath versus non-smokers as determined in a pilot study using PTR-MS. J. Breath Res. 2, 26002–26028. https://doi.org/10.1088/1752-7155/2/2/026002.

Lemmetty, M., Keskinen, J., Marjamäki, M., 2005. The ELPI response and data reduction II: properties of kernels and data inversion. Aerosol Sci. Technol. 39, 583–595. https://doi.org/10.1080/027868291009224.

Lindinger, W., Hansel, A., Jordan, A., 1998. On-line monitoring of volatile organic compounds at pptv levels by means of Proton-Transfer-Reaction Mass Spectrometry (PTR-MS) Medical applications, food control and environmental research. Int. J. Mass Spectr. Ion Proces. 173, 191–241. https://doi.org/10.1016/s0168-1176(97)00281-4.

Li, N., Georas, S., Alexis, N., Fritz, P., Xia, T., Williams, M.A., Horner, E., Nel, A., 2016. A work group report on ultrafine particles (American Academy of Allergy, Asthma & Immunology): why ambient ultrafine and engineered nanoparticles should receive special attention for possible adverse health outcomes in human subjects. J. Allergy Clin. Immunol. 138, 386–396. https://doi.org/10.1016/j.jaci.2016.02.023.

Maclean, R.R., Valentine, G.W., Jatlow, P.I., Sofuoglu, M., 2017. Inhalation of Alcohol Vapor: Measurement and Implications. https://doi.org/10.1111/acer.13291.

Malo, J.-L., Chan-Yeung, M., 2009. Agents causing occupational asthma. J. Allergy Clin. Immunol. 123, 545–550. https://doi.org/10.1016/J.JACI.2008.09.010.

Marjamäki, M., Keskinen, J., Chen, D.R., Pui, D.Y.H., 2000. Performance evaluation of the electrical low-pressure impactor (ELPI). J. Aerosol Sci. 31, 249–261. https://doi.org/10.1016/S0021-8502(99)00052-X.

Marjamäki, M., Lemmetty, Jorma Keskinen, M., 2005. ELPI response and data reduction I: response functions. Aerosol Sci. Technol. 39, 575–582. https://doi.org/10.1080/027868291009189.

Melchior Gerster, F., Brenna Hopf, N., Pierre Wild, P., Vernez, D., 2014. Airborne exposures to monoethanolamine, glycol ethers, and benzyl alcohol during professional cleaning: a pilot study. Ann. Occup. Hyg. 58, 846–859. https://doi.org/10.1093/ANNHYG/MEU028.

Meyers, C., Kass, R., Goldenberg, D., Milici, J., Alam, S., Robison, R., 2021. Ethanol and isopropanol inactivation of human coronavirus on hard surfaces. J. Hosp. Inf. 107, 45–49. https://doi.org/10.1016/j.jhin.2020.09.026.

Mouton, A.J., Maxi, J.K., Souza-Smith, F., Bagby, G.J., Gilpin, N.W., Molina, P.E., Gardner, J.D., 2016. Alcohol vapor inhalation as a model of alcohol-induced organ disease. Alcohol.: Clin. Exp. Res. 40, 1671–1678. https://doi.org/10.1111/acer.13133.

Msaada, K., Hosni, K., ben Taarit, M., Chahed, T., Kchouk, M.E., Marzouk, B., 2007. Changes on essential oil composition of coriander (Coriandrum sativum L.) fruits during three stages of maturity. Food Chem. 102, 1131–1134. https://doi.org/10.1016/j.foodchem.2006.06.046.

Nazarenko, Y., Han, T.W., Lioy, P.J., Mainelis, G., 2011. Potential for exposure to engineered nanoparticles from nanotechnology-based consumer spray products. J. Expos. Sci. Environmental Epidemiol. 21, 515–528. https://doi.org/10.1038/jes.2011.10.

Nematollahi, N., Kolev, S.D., Steinemann, A., 2018. Volatile chemical emissions from essential oils. Air Quality, Atmos. Health 11, 949–954. https://doi.org/10.1007/s11869-018-0606-0.

Nuyttens, D., Baetens, K., de Schampheleire, M., Sonck, B., 2007. Effect of nozzle type, size and pressure on spray droplet characteristics. Biosyst. Eng. 97, 333–345. https://doi.org/10.1016/j.biosystemseng.2007.03.001.

Oberdörster, G., 2000. Pulmonary effects of inhaled ultrafine particles. Int. Arch. Occup. Environ. Health. https://doi.org/10.1007/s004200000185.

Oberdörster, G., Oberdörster, E., Oberdörster, J., 2005. Nanotoxicology: an emerging discipline evolving from studies of ultrafine particles. Environ. Health Perspect. 113, 823–839. https://doi.org/10.1289/ehp.7339.

Pagonis, D., Sekimoto, K., de Gouw, J., 2019. A library of proton-transfer reactions of H_3O^+ ions used for trace gas detection. J. Am. Soc. Mass Spectr. 30, 1330–1335. https://doi.org/10.1007/s13361-019-02209-3.

Panas, A., Comouth, A., Saathoff, H., Leisner, T., Al-Rawi, M., Simon, M., Seemann, G., Dssel, O., Mlhopt, S., Paur, H.R., Fritsch-Decker, S., Weiss, C., Diabat, S., 2014. HEI perspectives 3: understanding the health effects of ambient ultrafine particles. Beilstein J. Nanotechnol. 5, 1590–1602.

Pitol, A.K., Julian, T.R., 2021. Community transmission of SARS-CoV-2 by surfaces: risks and risk reduction strategies. Environ. Sci. Technol. Lett. https://doi.org/10.1021/acs.estlett.0c00966 acs.estlett.0c00966.

Rabenau, H.F., Kampf, G., Cinatl, J., Doerr, H.W., 2005. Efficacy of various disinfectants against SARS coronavirus. J. Hosp. Infect. 61, 107–111. https://doi.org/10.1016/j.jhin.2004.12.023.

Saari, S., Arffman, A., Harra, J., Rönkkö, T., Keskinen, J., 2018. Performance evaluation of the HR-ELPI+ inversion. Aerosol Sci. Technol. 52, 1037–1047. https://doi.org/10.1080/02786826.2018.1500679.

Salthammer, T., 2016. Very volatile organic compounds: an understudied class of indoor air pollutants. Indoor Air 26, 25–38. https://doi.org/10.1111/ina.12173.

Schripp, T., Fauck, C., Salthammer, T., 2010. Interferences in the determination of formaldehyde via PTR-MS: what do we learn from m/z 31? Int. J. Mass Spectr. 289, 170–172. https://doi.org/10.1016/j.ijms.2009.11.001.

Soppa, V.J., Schins, R.P.F., Hennig, F., Hellack, B., Quass, U., Kaminski, H., Kuhlbusch, T. A.J., Hoffmann, B., Weinmayr, G., 2014. Respiratory effects of fine and ultrafine particles from indoor sources-a randomized sham-controlled exposure study of healthy volunteers. Int. J. Environ. Res. Public Health 11, 6871–6889. https://doi.org/10.3390/ijerph110706871.

Španěl, P., Smith, D., 2008. Quantification of trace levels of the potential cancer biomarkers formaldehyde, acetaldehyde and propanol in breath by SIFT-MS. J. Breath Res. 2, 46003. https://doi.org/10.1088/1752-7155/2/4/046003.

Španěl, P., Smith, D., 1998. Selected ion flow tube studies of the reactions of H_3O^+, NO^+, and O_2^+ with several aromatic and aliphatic hydrocarbons. Int. J. Mass Spectr. 181, 1–10. https://doi.org/10.1016/s1387-3806(98)14114-3.

Stone, V., Miller, M.R., Clift, M.J.D., Elder, A., Mills, N.L., Møller, P., Schins, R.P.F., Vogel, U., Kreyling, W.G., Jensen, K.A., Kuhlbusch, T.A.J., Schwarze, P.E., Hoet, P., Pietroiusti, A., de Vizcaya-Ruiz, A., Baeza-Squiban, A., Teixeira, J.P., Tran, C.L., Cassee, F.R., 2017. Nanomaterials versus ambient ultrafine particles: an opportunity to exchange toxicology knowledge. Environ. Health Perspect. https://doi.org/10.1289/EHP424.

U.S. Environmental Protection Agency (EPA), 2020. List N: Disinfectants for Coronavirus (COVID-19).

U.S. Environmental Protection Agency (EPA), 2011. Exposure Factors Handbook: 2011 Edition. Washington, DC.

Vizcaya Fernández, D., Mirabelli, M.C., Antó, J.M., Orriols, R., Burgos, F., Arjona, L., Zock, J.P., 2011. A workforce-based study of occupational exposures and asthma symptoms in cleaning workers. Occup. Environ. Med. 68, 914–919. https://doi.org/10.1136/OEM.2010.063271.

Wang, Lmei, Li, Mteng, Jin, Wwen, Li, S., Zhang, Sqi, Yu, Ljiang, 2009. Variations in the components of Osmanthus fragrans Lour. essential oil at different stages of flowering. Food Chem. 114, 233–236. https://doi.org/10.1016/j.foodchem.2008.09.044.

Weichenthal, S., Dufresne, A., Infante-Rivard, C., 2007. Indoor ultrafine particles and childhood asthma: exploring a potential public health concern. Indoor Air 17, 81–91. https://doi.org/10.1111/j.1600-0668.2006.00446.x.

Wilson, P.F., Freeman, C.G., McEwan, M.J., 2003. Reactions of small hydrocarbons with H_3O^+, O_2^+ and NO^+ ions. Int. J. Mass Spectr. 229, 143–149. https://doi.org/10.1016/S1387-3806(03)00290-2.

Wolkoff, P., Wilkins, C.K., Clausen, P.A., Nielsen, G.D., 2006. Organic compounds in office environments - sensory irritation, odor, measurements and the role of reactive chemistry. Indoor Air 16, 7–19. https://doi.org/10.1111/j.1600-0668.2005.00393.x.

Wu, T., Boor, B.E., 2020. Characterization of a thermal aerosol generator for HVAC filtration experiments (RP-1734). Sci. Technol. Built Environ. 26, 816–834. https://doi.org/10.1080/23744731.2020.1730661.

Yoon, H.I., Hong, Y.C., Cho, S.H., Kim, H., Kim, Y.H., Sohn, J.R., Kwon, M., Park, S.H., Cho, M.H., Cheong, H.K., 2010. Exposure to volatile organic compounds and loss of pulmonary function in the elderly. Eur. Respir. J. 36, 1270–1276. https://doi.org/10.1183/09031936.00153509.

Zhao, Q., Li, Y., Chai, X., Xu, L., Zhang, L., Ning, P., Huang, J., Tian, S., 2019. Interaction of inhalable volatile organic compounds and pulmonary surfactant: potential hazards of VOCs exposure to lung. J. Hazard. Mater. 369, 512–520. https://doi.org/10.1016/j.jhazmat.2019.01.104.

Zheng, G., Filippelli, G.M., Salamova, A., 2020. Increased indoor exposure to commonly used disinfectants during the COVID-19 pandemic. Environ. Sci. Technol. Lett. 7, 760–765. https://doi.org/10.1021/acs.estlett.0c00587.